

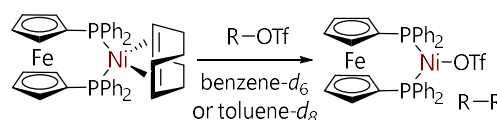
On the reactions of aryl and vinyl triflates with $[\text{Ni}(\text{COD})(\text{dppf})]^\ddagger$

Megan E. Greaves,^{a,b,†} Thomas O. Ronson,^b Stephen Sproules,^c and David J. Nelson^{*,a}

We report the experimental and computational investigations of the reactions of aryl and vinyl triflates with a model nickel(0) complex. Oxidative addition rates decrease in the order naphthyl > vinyl > phenyl, although 4-acetylphenyl triflate reacts most quickly due to favourable ketone coordination. Two possible reaction mechanisms are explored using DFT calculations.

Organotriflates are substrates for many nickel-catalysed reactions.^{1–6} The reactions of a range of Ni^0 complexes with organohalides have been studied in some depth,⁷ but less is known about the mechanisms of the reactions of aryl and vinyl triflates with Ni^0 . We have previously studied the reactions of a range of aryl (pseudo)halides with $[\text{Ni}(\text{COD})(\text{dppf})]$ (**1**),⁸ which is a convenient, thermally-stable, catalytically-active model nickel(0) complex (COD = 1,5-cyclooctadiene; dppf = 1,1'-bis(diphenylphosphino)ferrocene).⁹ We have studied the reactions of **1** with (hetero)aryl^{8, 10–12} and alkyl^{13, 14} halides, and ranked a series of aryl substrates of the form $p\text{-F}_3\text{CC}_6\text{H}_4\text{X}$ in order of their reactivity with **1**,⁸ somewhat surprisingly, **1** undergoes reaction with $p\text{-F}_3\text{CC}_6\text{H}_4\text{OTf}$ more slowly than with $p\text{-F}_3\text{CC}_6\text{H}_4\text{OTs}$. Recently, we noted that the reaction of 2-pyridyl triflate (**2a**) with **1** forms $[\text{Ni}(\kappa^2\text{-C},N\text{-2-pyridyl})(\text{dppf})][\text{OTf}]$ in which the triflate moiety is present as an outer-sphere counterion to a pseudo-square planar cationic nickel(II) complex.¹¹ Neufeldt noted that selectivity for aryl sulfonate *versus* aryl chloride oxidative addition can be modulated *via* judicious ligand selection: Ni^0 complexes with most widely-used phosphine ligands preferentially activate aryl chlorides, while complexes of trimethylphosphine show the opposite selectivity by lowering the energy of the five-centre oxidative addition transition state for aryl triflate oxidative addition.¹⁵ Here we examine the reactions of a series of aryl and vinyl triflates with **1**.

The reactions of **1** with phenyl (**2b**), 2-naphthyl (**2d**), or cycloalk-1-en-1-yl triflates (cyclopent-1-en-1-yl triflate (**3a**), cyclohex-1-en-1-yl triflate (**3b**), cyclohept-1-en-1-yl triflate (**3c**), and cyclooct-1-en-1-yl triflate (**3d**)) ultimately form $[\text{Ni}(\text{OTf})(\text{dppf})]$ (**4**) (Scheme 1), as confirmed by EPR analysis



Scheme 1. Product studies for the reaction of $[\text{Ni}(\text{COD})(\text{dppf})]$ (**1**) with organotriflates.

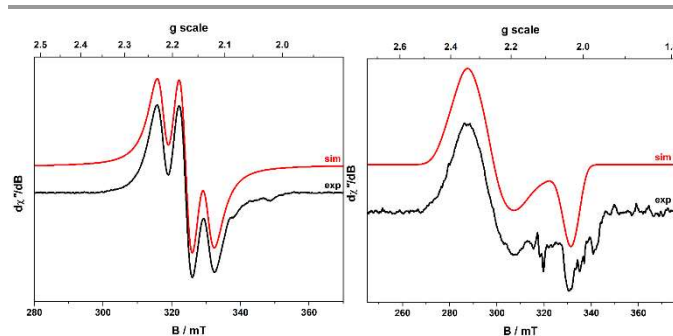


Figure 1. X-band EPR spectra of $[\text{Ni}(\text{OTf})(\text{dppf})]$ (**4**) in THF solution (left) at 293 K (frequency, 9.8593 GHz; power, 6.3 mW; modulation, 0.6 mT) showing $g_{\text{iso}} = 2.173$ and $A_{\text{iso}} = 65 \times 10^{-4} \text{ cm}^{-1}$ and (right) at 77K (frequency, 9.4215 GHz; power, 2.0 mW; modulation, 0.7 mT) showing $g = (2.340, 2.265, 2.035)$ and $A = (80, 80, 30) \times 10^{-4} \text{ cm}^{-1}$. Experimental spectra are in black (bottom) and simulations are shown in red (at the top).

(Figure 1). The corresponding reactions with 1-naphthyl triflate (**2c**) and 4-(trifluoromethyl)phenyl triflate (**2e**) are known to lead to $[\text{Ni}(1\text{-naphthyl})(\text{OTf})(\text{dppf})]$ (**4**) and **2**, respectively.⁸ Homocoupling by-products were identified by GC-MS analysis; in the case of the reactions of **3a**, the identity of this by-product was confirmed by the analysis of an authentic sample.⁵

Kinetic studies of the oxidative addition step were performed by monitoring the decrease in the concentration of **1** over time by $^{31}\text{P}\{\text{H}\}$ NMR spectroscopy when it was exposed to **2a-d**, **2f**, and **3a-d** in benzene- d_6 solution under an argon atmosphere (Scheme 2).⁵ The rate of reaction decreases in the order 2-naphthyl > 4-acetylphenyl \approx 1-naphthyl > 2-pyridyl > phenyl. The increased rate of reaction of heteroaryl halides compared to aryl halides has been noted previously in the oxidative addition reactions of nickel¹¹ and palladium.¹⁶ The increased reactivity of **2f** with respect to **2b** is consistent with our previous studies, in which ketone coordination accelerates oxidative addition when 'ring-walking' across the π -system is possible;^{10, 12} the present study establishes that this behaviour extends beyond aryl halides to other nickel catalysis substrates.

Intrigued by the possible role of alkene coordination in reaction rate and selectivity,^{10, 12} four vinyl triflate substrates were prepared from the corresponding cycloalkanone.^{5,5}

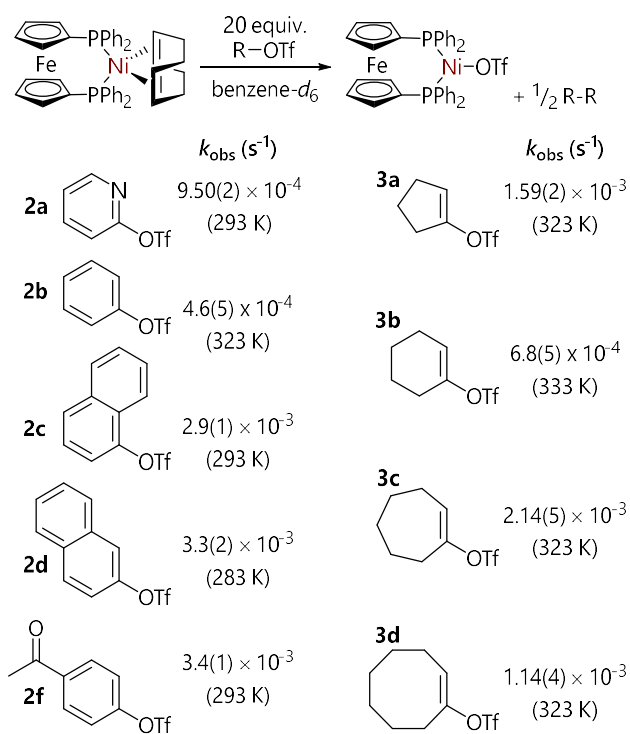
^a WestCHEM Department of Pure & Applied Chemistry, University of Strathclyde, 295 Cathedral Street, Glasgow, G1 1XL, Scotland. david.nelson@strath.ac.uk

^b Chemical Development, Pharmaceutical Technology & Development, Operations, AstraZeneca, Macclesfield, SK10 2NA, UK.

^c WestCHEM School of Chemistry, University of Glasgow, University Avenue, Glasgow, G12 9QQ, Scotland.

[†] Current address: Department of Chemistry, Massachusetts Institute of Technology, 77 Massachusetts Avenue, Cambridge, MA 02139, USA.

Electronic Supplementary Information (ESI) available: characterisation data for chemical compounds, kinetic data, and information about computational calculations.



Scheme 2. Kinetic studies of the oxidative addition of aryl and vinyl triflates to **1**.

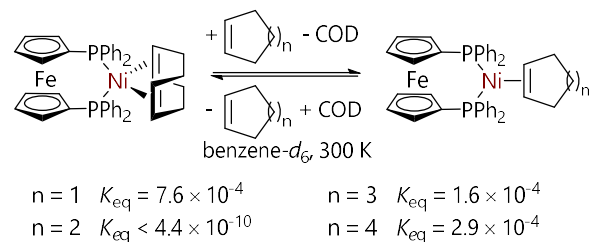
Substrates **3a**, **3c**, and **3d** undergo reaction at *ca.* two to four times the rate of phenyl triflate. However, cyclohex-1-en-1-yl triflate (**3b**) undergoes reaction at *ca.* half the rate of phenyl triflate (**2b**), for which $k_{obs} = 1.3(1) \times 10^{-3}$ at 333 K. This anomalous result was explored further (*vide infra*).

The reactions of **2b** and **3a** were repeated with the addition of 1, 2, or 3 equivalents of COD; in both cases the rate of reaction decreased with increasing $[COD]_{t=0}$ consistent with the need to generate a vacant site for oxidative addition.⁵

The surprisingly low rate of oxidative addition for **3b** prompted further investigation. Equilibrium constants were measured by $^{31}P\{^1H\}$ NMR spectroscopy for the displacement of COD from **1** by cyclopentene, cyclohexene, cycloheptene, and *cis*-cyclooctene (Scheme 3); we have previously shown that ketones and aldehydes can coordinate to dppf-nickel(0),¹⁰ even displacing good ligands such as COD, and we have noted that a whole range of coordinating functional groups affect the outcomes of nickel-catalysed Suzuki-Miyaura cross-coupling reactions.¹² The data in Scheme 3 show that K_{eq} decreases in the order cyclopentene > *cis*-cyclooctene > cycloheptene >> cyclohexene. The reticence of **3b** to engage in oxidative addition with **1** may be due to less favourable substrate coordination to the dppf-Ni⁰ complex.

Computational studies, for which full details can be found in the supporting information,⁵ were used to further explore these reactions. Calculations were carried out at the MN15/6-311+G(d,p)/SMD(benzene)//B3LYP-D3/6-31G(d)+LANL2TZ(f) level of theory. This level of theory was benchmarked against DLPNO-CCSD(T)/cc-pVTZ/SMD(benzene) calculations.⁵

The exchange of COD for a cycloalkene at [Ni(dppf)] was explored first. The value of ΔG° increased in the order cyclopentene (3.4 kcal/mol; $K_{eq} = 3 \times 10^{-3}$) < *cis*-cyclooctene (3.8 kcal/mol; $K_{eq} = 2 \times 10^{-3}$) < cycloheptene (5.4 kcal/mol; $K_{eq} = 1 \times$



Scheme 3. Measurement of K_{eq} for the displacement of COD from **1** by cycloalkenes.

10^{-4}) << cyclohexene (7.4 kcal/mol; $K_{eq} = 4 \times 10^{-6}$), entirely consistent with the order of K_{eq} obtained experimentally.

The oxidative addition reactions proceed *via* displacement of COD from **1** by the substrate to form an intermediate η^2 -complex, followed by oxidative addition *via* an S_N -type or five-centre transition state. The S_N -type transition states exhibit Ni...C interactions but no Ni...O interactions, while the latter show Ni...C and Ni...O interactions, as judged by QTAIM.⁵ The profiles for the oxidative addition of phenyl, 1-naphthyl, and 2-naphthyl triflate (**2b-d**) are shown in Figure 2(a)-(c), as well as structures of the S_N -type and five-centre transition states. The two possible oxidative addition transition states for **2b** are within 1 kcal/mol, but naphthyl systems show a small preference for a five-centre transition state. These calculations correctly rank the aryl triflate substrates in order of reactivity, but somewhat overestimate the differences in reaction rate ($k_{rel} = 5 \times 10^4 : 6 \times 10^2 : 1$ for **2d** : **2c** : **2b**), assuming that the reaction rates approximately double for every 10 K increase in temperature.

The computational modelling of the reactions of *cis*-cycloalk-1-en-1-yl triflates are complicated by the various conformations that cycloalkenes can adopt.^{17, 18} Data reported here are for the lowest energy pathway for each substrate (Figure 2).⁵⁵ The formation of an η^2 -substrate complex ranges from slightly endergonic to slightly exergonic ($G_{rel} = 0.7$ to -2.8 kcal/mol). In most cases, the most favourable pathway for oxidative addition is *via* **TS**⁵, with the exception of cyclohex-1-en-1-yl triflate (**3b**). DFT calculations suggest that the barrier to oxidative addition decreases in the order **3a** (12.6 kcal/mol) > **3b** (9.5 kcal/mol) > **3c** (7.1 kcal/mol) > **3d** (6.2 kcal/mol).⁵⁵⁵ The calculations therefore correctly rank three of the four substrates in the order of their reactivity.

A representative set of aryl and vinyl triflates was deployed in Kumada-Tamao-Corriu cross-coupling reactions to confirm that **1** is a competent catalyst for the cross-coupling reactions of these substrates (Scheme 4(a); Table 1). These conditions are unoptimised, but were previously deployed for the cross-coupling of alkyl halides with aryl Grignard reagents, and use only 1.1 equivalents of the latter.^{13, 14} Reaction yields were quantified by GC-FID analysis using an internal standard, which was calibrated using authentic samples of each product; a substituted aryl triflate (**2g**) was used rather than **2a** in order to distinguish between cross- and homo-coupling processes. The reactions proceeded in moderate to excellent yields, confirming the competence of this catalyst system. There is not a correlation between oxidative addition rate and reaction yield, but these are single point yield measurements from catalytic reactions carried out at a higher temperature and for a longer

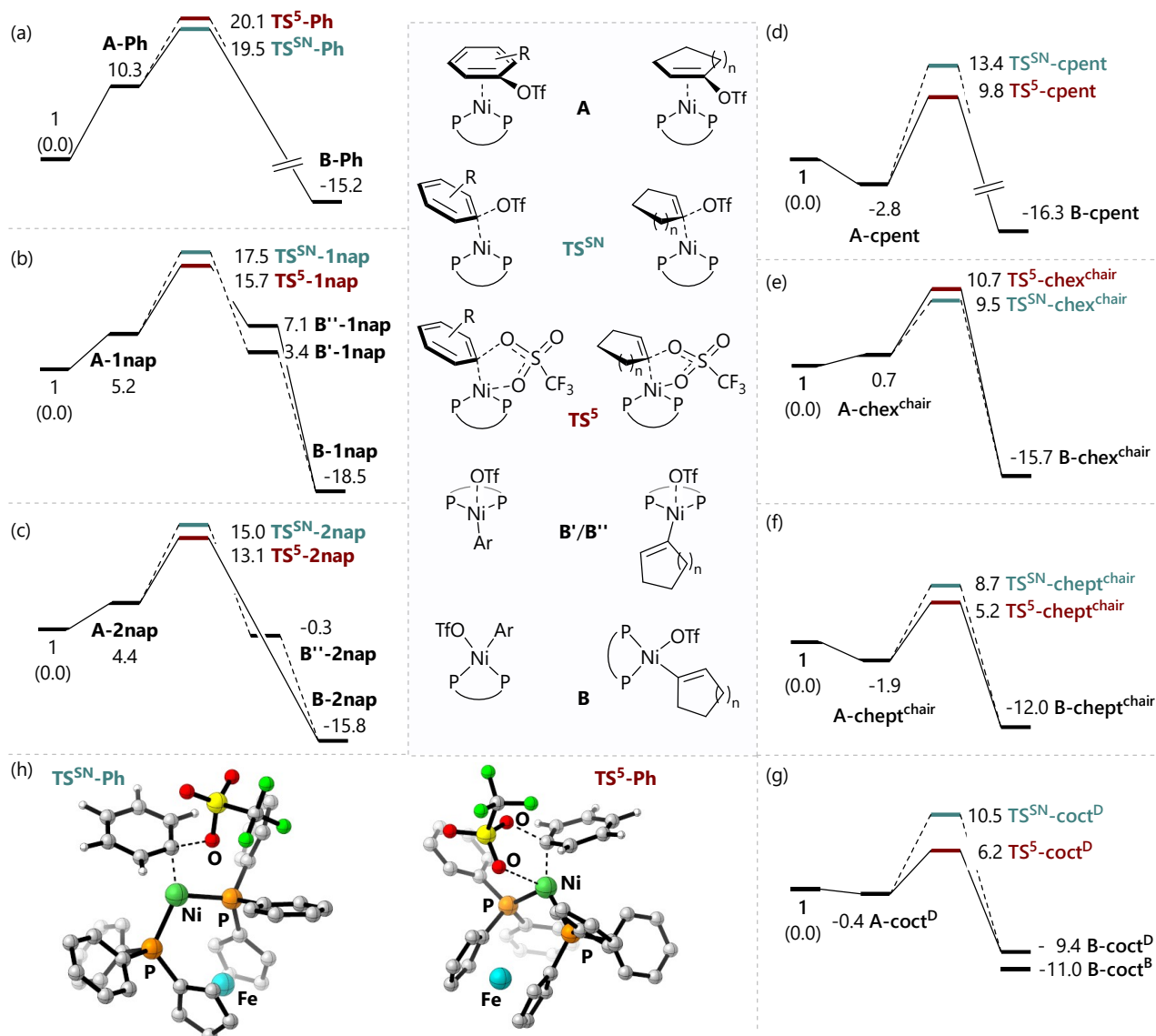
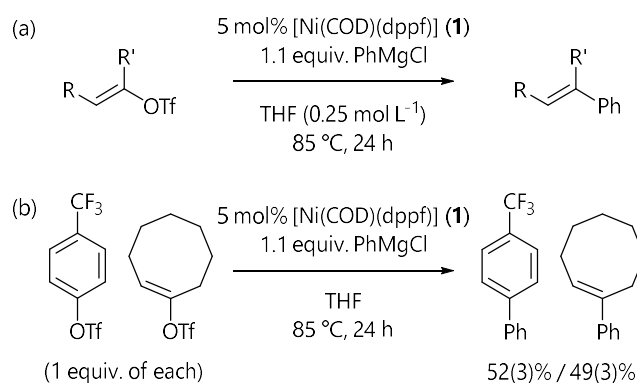


Figure 2. Free energy profiles at MN15/6-311+G(d,p)/SMD(benzene)//B3LYP-D3/6-31G(d)+LANL2TZ(f) for the oxidative addition reactions of complex **1** with (a) phenyl triflate (**2b**), (b) 1-naphthyl triflate (**2c**), (c) 2-naphthyl triflate (**2d**), (d) cyclopent-1-en-1-yl triflate (**3a**), (e) cyclohex-1-en-1-yl triflate (**3b**), (f) cyclohept-1-en-1-yl triflate (**3c**) and (g) cyclooct-1-en-1-yl triflate (**3d**). (h) S_N -type (left) and five-centre (right) transition states for the oxidative addition of phenyl triflate (**2b**) to $[\text{Ni}(\text{COD})(\text{dppf})]$ (**1**).

time period than the oxidative addition studies. The rather low yield of 1-phenyl-cyclopentene is an outlier, and the fate of the missing 45% of the substrate is unclear at this stage; this may be due to formation of cyclopentene, which is sufficiently volatile to be lost in the solvent front during GC-FID analysis.

Finally, we wished to identify whether the more favourable coordination of vinyl triflates to Ni^0 (compared to aryl triflates) might allow a selective cross-coupling reaction to be achieved. Reactions were carried out in which one equivalent of each of 4-(trifluoromethyl)phenyl triflate and cyclooct-1-en-1-yl triflate were exposed to 1.1 equivalents of phenylmagnesium chloride and 5 mol% of $[\text{Ni}(\text{COD})(\text{dppf})]$; these reactions were unselective, and produced the corresponding products in approximately equal yield (Scheme 4(b)).



Scheme 4. Prototypical Kumada-Tamao-Corriu cross-coupling reactions.

Table 1. Outcomes of Kumada-Tamao-Corriu Cross-Coupling Reactions^a

Substrate	Conversion	Yield
Cyclopent-1-en-1-yl Triflate (3a)	95%	50(2)%
Cyclohex-1-en-1-yl Triflate (3b)	100%	85(1)%
Cyclohept-1-en-1-yl Triflate (3c)	100%	87(5)%
Cyclooct-1-en-1-yl Triflate (3d)	100%	96%
<i>para</i> -(Trifluoromethyl)phenyl triflate (2g)	90(3)%	79(1)%

a) All reactions were conducted in duplicate under the conditions noted in Scheme 4, and results are reported as the average of two replicates. Yields determined by calibrated GC-FID analysis using an internal standard.⁵

In conclusion, we have systematically studied the reactions of a model Ni⁰ complex with aryl and vinyl triflates. The preference for S_N-type *versus* five-centre oxidative addition transition states is a function of the substrate. The order of reactivity is approximately naphthyl > 2-pyridyl > vinyl > phenyl. The coordination of vinyl substrates to Ni⁰ is likely to play a key role in determining the rate of oxidative addition but does not appear to enable vinyl-over-aryl selectivity.

We thank AstraZeneca and the Engineering and Physical Sciences Research Council for an Industrial CASE Studentship for M.E.G.. We thank Mr C. Irving, Ms P. Keating, and Mr F. McGeoch for assistance with technical and analytical facilities at the University of Strathclyde. Some of the calculations were performed using the Archie-WEST High Performance Computer (archie-west.strath.ac.uk) at the University of Strathclyde, and we thank Mr J. Buzzard, Dr K. Kubiak-Ossowska, and Dr R. Martin for assistance with this facility.

Author Contributions

M.E.G.: data curation; formal analysis; investigation; methodology; writing – original draft. S.S.: data curation; formal analysis; investigation; methodology; resources. T.O.R.: funding acquisition; project administration; supervision. D.J.N.: conceptualisation; data curation; formal analysis; funding acquisition; investigation; methodology; project administration; resources; supervision; visualisation; writing – original draft; writing – review & editing.

Notes and references

‡ Dedicated to Patricia Keating on her retirement after 40 years working within the Department of Pure & Applied Chemistry.

§ See the Supporting Information for full details.

§§ Conformations were generated based on the literature and/or using CREST/xTB. Pathways for each conformation are reported in the supporting information,⁵ and were explored in case the lowest energy pathway involved a conformational change.

§§§ It is unclear why the results for **3a** are not consistent with experimental observations. Repeated attempts to find alternative, lower-energy transition states were unsuccessful.

1. H. Chen, S. Sun and X. Liao, *Org. Lett.*, 2019, **21**, 3625-3630.
2. F.-F. Pan, P. Guo, C.-L. Li, P. Su and X.-Z. Shu, *Org. Lett.*, 2019, **21**, 3701-3705.
3. L. Su, G. Ma, Y. Song and H. Gong, *Org. Lett.*, 2021, **23**, 2493-2497.
4. X. Wang, F. Liu, Z. Yan, Q. Qiang, W. Huang and Z.-Q. Rong, *ACS Catal.*, 2021, **11**, 7319-7326.
5. J. Duan, Y.-F. Du, X. Pang and X.-Z. Shu, *Chem. Sci.*, 2019, **10**, 8706-8712.

6. Z.-X. Tian, J.-B. Qiao, G.-L. Xu, X. Pang, L. Qi, W.-Y. Ma, Z.-Z. Zhao, J. Duan, Y.-F. Du, P. Su, X.-Y. Liu and X.-Z. Shu, *J. Am. Chem. Soc.*, 2019, **141**, 7637-7643.
7. M. E. Greaves, E. L. B. Johnson Humphrey and D. J. Nelson, *Catal. Sci. Technol.*, 2021, **11**, 2980-2996.
8. S. Bajo, G. Laidlaw, A. R. Kennedy, S. Sproules and D. J. Nelson, *Organometallics*, 2017, **36**, 1662-1672.
9. G. Yin, I. Kalvet, U. Englert and F. Schoenebeck, *J. Am. Chem. Soc.*, 2015, **137**, 4164-4172.
10. A. K. Cooper, D. K. Leonard, S. Bajo, P. M. Burton and D. J. Nelson, *Chem. Sci.*, 2020, **11**, 1905-1911.
11. A. K. Cooper, M. E. Greaves, W. Donohoe, P. M. Burton, T. O. Ronson, A. R. Kennedy and D. J. Nelson, *Chem. Sci.*, 2021, **12**, 14074-14082.
12. A. K. Cooper, P. M. Burton and D. J. Nelson, *Synthesis*, 2020, **52**, 565-573.
13. M. E. Greaves, T. O. Ronson, F. Maseras and D. J. Nelson, *Organometallics*, 2021, **40**, 1997-2007.
14. M. E. Greaves, T. O. Ronson, G. C. Lloyd-Jones, F. Maseras, S. Sproules and D. J. Nelson, *ACS Catal.*, 2020, **10**, 10717-10725.
15. E. D. Entz, J. E. A. Russell, L. V. Hooker and S. R. Neufeldt, *J. Am. Chem. Soc.*, 2020, **142**, 15454-15463.
16. B. U. W. Maes, S. Verbeeck, T. Verhelst, A. Ekomié, N. von Wolff, G. Lefèvre, E. A. Mitchell and A. Jutand, *Chem. Eur. J.*, 2015, **21**, 7858-7865.
17. D. J. Nelson, I. W. Ashworth, I. H. Hillier, S. H. Kyne, S. Pandian, J. A. Parkinson, J. M. Percy, G. Rinaudo and M. A. Vincent, *Chem. Eur. J.*, 2011, **17**, 13087-13094.
18. U. Neuenschwander and I. Hermans, *J. Org. Chem.*, 2011, **76**, 10236-10240.
19. M. Álvarez-Moreno, C. de Graaf, N. López, F. Maseras, J. M. Poblet and C. Bo, *J. Chem. Inf. Model.*, 2015, **55**, 95-103.